

Federated Learning Over Cellular-Connected UAV Networks with Non-IID Datasets

Di-Chun Liang[†], Chun-Hung Liu[‡], Rung-Hung Gau[†], and Lu Wei^{*}

Institute of Communications Engineering, National Yang Ming Chiao Tung University, Hsinchu, Taiwan[†]

Department of Electrical and Computer Engineering, Mississippi State University, USA[‡]

Department of Computer Science, Texas Tech University, Lubbock TX, USA^{*}

e-mail: ldc.cm02g@nctu.edu.tw[†]; chliu@ece.msstate.edu[‡]; runghunggau@g2.nctu.edu.tw[†]; luwei@ttu.edu^{*}

Abstract—Federated learning (FL) is a promising distributed learning technique particularly suitable for wireless learning scenarios since it can accomplish a learning task without raw data transportation so as to preserve data privacy and lower network resource consumption. However, current works on FL over wireless communication do not profoundly study the fundamental performance of FL that suffers from data delivery outage due to network interference and data heterogeneity among mobile clients. To accurately exploit the performance of FL over wireless communication, this paper proposes a new FL model over a cellular-connected unmanned aerial vehicle (UAV) network, which characterizes data delivery outage from UAV clients to their server and data heterogeneity among the datasets of UAV clients. We devise a simulation-based approach to evaluating the convergence performance of the proposed FL model. We then propose a tractable analytical framework of the uplink outage probability in the cellular-connected UAV network and derive a neat expression of the uplink outage probability, which reveals how the proposed FL model is impacted by data delivery outage and UAV deployment. Extensive numerical simulations are conducted to show the consistency between the estimated and simulated performances.

I. INTRODUCTION

In the recent years, we have witnessed that machine learning (ML) techniques have been dramatically improved and successfully applied to tackle many real-world problems. The remarkable success of ML is mainly attributed to two key factors – highly powerful computing and extremely efficient data analytics, yet such a remarkable progress in ML significantly relies on whether or not there are enough data to support ML algorithms so as to make them work desirably, which becomes a crucial issue in many ML applications. Due to the proliferation of smart mobile devices, collecting data through them becomes much feasible and easier such that a mobile cellular network has gradually been a huge live database abounding with real-time information, which can be utilized by ML to optimize network operations and managements. Proper and efficient utilization of ML techniques from data distributed over a massive mobile network becomes an important issue. This is especially true when transporting raw data from all mobile devices to a server with learning facilities that may cause issues such as network congestion, energy consumption, and security. To avoid the impractical tasks of transporting massive distributed data for centralized ML, distributed learn-

ing methodology without raw data transportation, such as the recently proposed federated learning (FL) [1], [2], [3], becomes a viable solution.

A number of the existing FL algorithms were developed with uniformly compressible data and shown to achieve convergence based on the assumption of error-free and reliable data communications between a server and clients. For example, reference [4] proposed a compression protocol that inherits the compression techniques of top- k sparsification and quantization for uplink and downlink communication in FL, where the distribution of datasets of each client are non-i.i.d. In [5], FL-based multi-access edge computing was studied with limited network resources, which adopted a gradient descent approach to find the optimal trade-off between local update at clients and global aggregation at a server. There are also a number of works in the recent years studying the problem of FL over wireless communication, where many of them approached the problem from the perspective of signal processing. The authors of reference [6], for instance, devised a compressive sensing approach for FL over single-antenna communication systems. The authors of reference [7] proposed a compressive sensing approach for FL over a MIMO communication system, where the server recursively finds the linear minimum-mean-square-error estimate of the transmitted signal by exploiting the sparsity of the signal. In [8], the authors studied the over-the-air computation (AirComp, proposed in [9]) problem with one-bit broadband digital aggregation. Furthermore, FL over UAV networks has been investigated in some prior works, such as [10].

In these prior works, a fundamental issue of FL over wireless communication is far from being fully resolved, that is, data communications between clients and a server may fail due to unreliable wireless transmissions, which leads to transmission outage and degrade the convergence performance of FL accordingly. Another crucial issue that is not addressed much in the prior works is the heterogeneity of datasets among different mobile clients. Namely, most of the existing works focus on developing wireless FL algorithms by assuming that all mobile clients possess independent and identically distributed (i.i.d.) datasets. To tackle these two issues, in this paper our first contribution is to propose a more realistic FL model that can characterize the transmission outages

between a server and mobile clients and be implemented in a cellular-connected UAV networks in which the datasets at all UAV clients are non-i.i.d. Our second contribution is to propose a tractable framework of evaluating the convergence performance of the proposed FL model from a network-wide perspective. A three-dimensional (3D) random deployment model is properly devised for modeling the random locations of UAV clients and access points (APs), which is the third contribution. Our fourth contribution is to conduct intensive numerical simulations in order to validate the correctness of our analytical findings and importantly demonstrate that the convergence performance of FL over wireless communication is fairly sensitive to data delivery outage as well as non-i.i.d. data nature. Moreover, the numerical results also shed light on the fundamental interplay between the deployment of UAVs and the learning accuracy of the proposed FL model.

II. FEDERATED LEARNING MODEL OVER CELLULAR-CONNECTED UAVS

In this paper, our main goal is to study the performance of FL over a cellular-connected UAV network consisting of numerous UAVs, APs, an edge server (ES), and a cloud. All the APs in the network are governed by an ES connected to a cloud through a gateway. The ES communicates with the cloud whenever it needs to send data for further large-scale data processing and learning. Each UAV associates with its strongest AP and conducts FL with the ES. An illustration of the proposed model is shown in Fig. 1(a). In the following, we will first propose an FL model with intermittent updates. Afterwards, some preliminary simulation results will be provided to illustrate how the proposed FL is affected by uplink transmission outages.

A. Proposed Federated Learning with Intermittent Updates

Now consider the network in Fig. 1(a) that is comprised of an ES communicating with multiple UAVs. In this network, there are C UAVs that would like to jointly learn a global model with an ES through their nearby AP in T training rounds. Since the wireless communications between the AP and each UAV are not reliable, data delivery outages would happen between the ES and each UAV, and they thus impact the performance of FL because the learning updates at the ES and the UAVs are intermittent. To characterize the impact of data delivery outage on FL between the ES and a UAV as well as tractably analyze the performance of FL with intermittent updates, data delivery outage is assumed to only happen in the uplink transmission from a UAV to its associated AP, yet the downlink transmission from the AP to a UAV is assumed to be outage-free. As such, we propose the FL with intermittent uplink outages as shown in Algorithm 1.

In Algorithm 1, each UAV U_i is assumed to possess a dataset \mathcal{D}_i given by

$$\mathcal{D}_i \triangleq \{D_j = (x_j, y_j), j \in \mathbb{N}_+\}, \quad \forall i \in \mathbb{N}_+, \quad (1)$$

⁰Note that all the UAVs joining the learning process can be in different cells, that is, these C UAVs may not associate with the same AP.

Algorithm 1 Federated Learning with Intermittent Updates

- 1: **inputs:** initial model vector w_o
 - 2: **outputs:** improved model vector w
 - 3: **initialize:** the global model is initialized as $w_0 \leftarrow w_o$. Each client holds non-i.i.d. dataset \mathcal{D}_i with equal size. $\nabla w_0, \nabla w_{i,0} \leftarrow 0$.
 - 4: **for** $t = 1, \dots, T$ **do**
 - 5: **for** $i \in \{1, \dots, C\}$ **do in parallel**¹
 - 6: client i does:
 - 7: · $w_{i,t} \leftarrow \text{download}_{i \leftarrow S}(w_{t-1})$
 - 8: · $\nabla w_{i,t} \leftarrow \sum_{j \in \mathcal{D}_i} \text{SGD}(D_j, w_{i,t}) - w_{i,t}$
 - 9: · $\text{upload}_{S \leftarrow i}(\nabla w_{i,t})$
 - 10: **end for**
 - 11: edge server does:
 - 12: · $\nabla w_t \leftarrow \frac{1}{\sum_{i \in \mathcal{D}} \beta_{i,t} |\mathcal{D}_i|} \sum_{i \in \mathcal{D}} \beta_{i,t} |\mathcal{D}_i| \nabla w_{i,t}$
 - 13: · $w_t \leftarrow w_{t-1} + \nabla w_t$
 - 14: · $w \leftarrow w_t$
 - 15: · $\text{broadcast}_{i \leftarrow S}(w_t)$
 - 16: **end for**
 - 17: **return** w
-

where D_j denotes data point j in set \mathcal{D}_i , x_i is the input data with an appropriate dimension, y_i is the labeled scalar output corresponding to x_i . All the datasets \mathcal{D}_i 's are assumed to be non-i.i.d. and of the same size in this paper. Note that each UAV and the ES initiate their own algorithm with the same initial model vector, i.e., $w_{i,0} \leftarrow w_o$ and $w_0 \leftarrow w_o$. All the UAVs are assumed to synchronously update their own local learning models. At the t th round of communication, client i updates its local model vector $w_{i,t}$ according to the following algorithm:

$$\begin{cases} w_{i,t} \leftarrow \text{download}_{i \leftarrow S}(w_{t-1}) \\ \nabla w_{i,t} \leftarrow \sum_{j \in \mathcal{D}_i} \text{SGD}(D_j, w_{i,t}) - w_{i,t} \end{cases}, \quad (2)$$

where $\text{SGD}(D_j, w_{i,t})$ stands for the calculation of Stochastic Gradient Descent with data point D_j and model vector $w_{i,t}$. After receiving the global model vector w_{t-1} from the ES broadcasted by the AP, UAV U_i updates its local model vector $w_{i,t}$ by SGD so as to find the gradient $\nabla w_{i,t}$. Subsequently, UAV U_i uploads the gradient $\nabla w_{i,t}$ to the ES through AP. To characterize the data delivery outage from U_i to AP, we adopt a Bernoulli random variable $\beta_{i,t} \in \{0, 1\}$ to model the uplink outage transmission from the UAV U_i to the AP at the t th round. Thus, the data aggregation algorithm at the ES can be expressed as

$$\begin{cases} \nabla w_t \leftarrow \frac{1}{\sum_{D_i \in \mathcal{D}} \beta_{i,t} |\mathcal{D}_i|} \sum_{D_i \in \mathcal{D}} \beta_{i,t} \nabla w_{i,t} \\ w_t \leftarrow w_{t-1} + \nabla w_t \end{cases}, \quad (3)$$

where $\mathcal{D} = \bigcup_i \mathcal{D}_i$. The ES aggregates the received gradients to ∇w_t by averaging all the received gradients from the UAVs[2]. As aforementioned, some gradients may be lost due to uplink outage transmissions so that the server is merely able to aggregate the gradients of the local model vectors successfully transmitted. The global model vector w_t at the

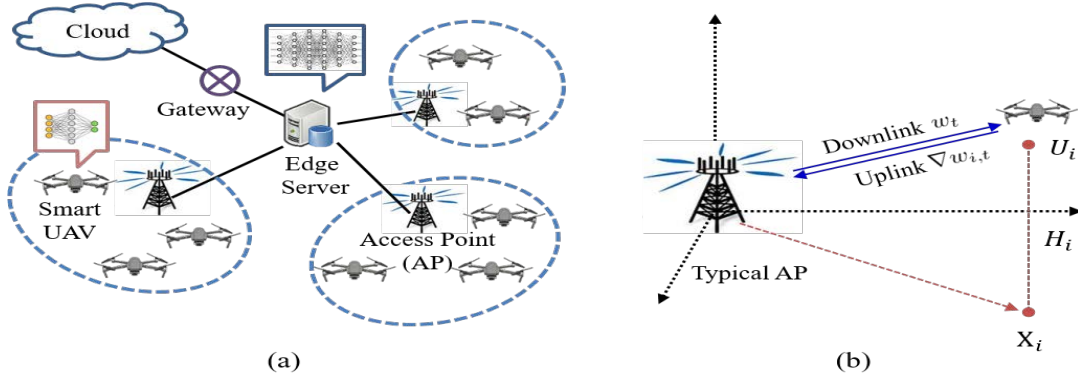


Fig. 1. (a) A cellular-connected UAV network consisting of numerous UAVs (users), APs, an edge server, and a cloud. Each UAV associates a nearby AP so as to perform the proposed FL algorithm (Algorithm 1) with the edge server. (b) An illustration shows that the typical AP located at the origin is associated with the UAV U_i .

t th round is then updated and subsequently broadcasted to the UAVs in the next round until the predesignated training round number T is reached. To illustrate how the proposed FL model in Algorithm 1 is impacted by uplink transmission outage, a preliminary simulation is provided in the following subsection in order to observe the convergence performance of the proposed FL model with intermittent updates.

B. A Numerical Glance of the Proposed FL Model

In this section, we provide a preliminary numerical illustration regarding how the convergence of the proposed FL model is influenced by uplink outages in a predesignated training round $T = 200$, as shown in Figs. 2(a) and 2(b). All the UAVs are assumed to experience the same uplink outage probability $p_{out} \triangleq \mathbb{P}[\beta_{i,t} = 0]$ and have the same capability of assembling data, i.e., the quality and size of the data collected by each UAV are identical. Moreover, we adopt the training data that are hand-written digit images from the famous MNIST dataset and evaluate the learning convergence by using the *accuracy* defined as the rate of successfully classifying the images in the entire dataset² by using the global model w found by the proposed FL model. To compare the results in the simulation, the UAVs perform SGD with the same model architecture that has equal batch sizes and the number of hidden layers and nodes. Each case terminates the learning process once reaching training round T . For the case of non-i.i.d. datasets, each UAV collects one specific class of the dataset where the ratio of data sizes for training and testing is 2:1. For the case of i.i.d. datasets, all the classes of the dataset are gathered by each UAV with the same probability. To make each case fairly comparable, the total data of each class for training are of the same size in order to make each class of data fairly trained. For example, if 50 UAVs are involved in the training, exactly 5 UAVs out of them gather the images of hand-written “3”, and so forth for other images of hand-written digit.

According to Algorithm 1, the global model vector w is directly affected by the number C of UAV clients and the uplink outage indicator $\beta_{i,t}$. Specifically, when the density of

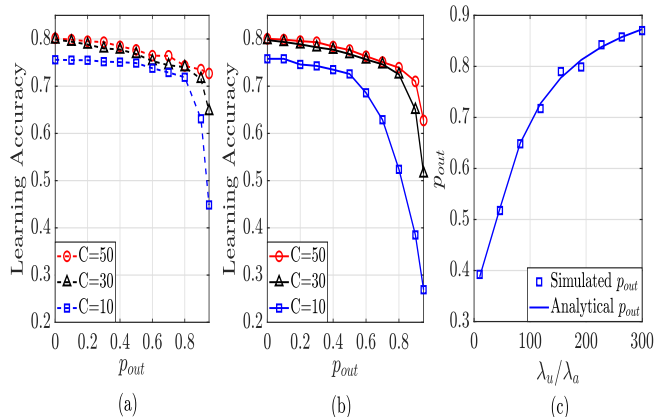


Fig. 2. The simulation results of the proposed FL model: (a) Uplink outage probability versus learning accuracy for different numbers of C UAV clients with i.i.d. datasets; (b) Uplink outage probability versus learning accuracy for different numbers of C UAV clients with non-i.i.d. datasets; (c) Uplink outage probability versus the ratio of the UAV density to the AP density.

the UAV increases, the number of clients C participating FL increases so that the rate of convergence increases as well, yet it could induce the risk of overfitting and increase the interference. According to Figs. 2(a) and 2(b), the accuracy degrades as p_{out} increases since the uploaded gradients are more likely to undergo transmission outage. Note that the impact of p_{out} is more severe when the UAVs have non-i.i.d. datasets. In contrast, the impact of p_{out} is less severe if the UAV possess i.i.d. datasets since any one of the UAVs that are able to successfully transmit can improve the FL process in each round. On the other hand, properly increasing the number of UAV clients helps FL and also provide some robustness to uplink outage. This simulation provides an overview for the influences of intermittent updates given uplink outage probabilities. It is important to point out that the distribution of the Bernoulli random process $\beta_{i,t}$ is impacted by the deployment densities of the UAVs and APs in the network in that it depends on the uplink interference dominated by the densities of the UAVs and APs. To exploit the fundamental relationship between the UAV and AP densities and the distribution of $\beta_{i,t}$, a cellular-connected UAV deployment model is proposed

²The entire dataset is the union of the local datasets at the UAVs.

in the following section.

III. SYSTEM MODEL AND OUTAGE ANALYSIS FOR CELLULAR-CONNECTED UAV NETWORKS

To demonstrate how the uplink transmission outage is affected by UAV and AP deployments and channel fading, in this section, we propose a UAV deployment model in which tractable analyses of the uplink outage probability can be conducted.

A. Deployment Model of Cellular-Connected UAVs

We assume all the UAV can be deployed according to the following 3D point process³:

$$\Phi_u \triangleq \{U_i \in \mathbb{R}^2 \times \mathbb{R} : U_i = (X_i, H_i), i \in \mathbb{N}_+\}, \quad (4)$$

where U_i , denotes UAV i and its 3D location, X_i is the projection of U_i on the plane of \mathbb{R}^2 , and H_i is the altitude of U_i , as depicted in Fig. 1(b). Note that the set of projections $\{X_i\}$ form a 2D homogeneous Poisson point process (PPP) of density λ_u . Similarly, all the APs in the network are assumed to form an independent 2D homogeneous PPP of density λ_a given by

$$\Phi_a \triangleq \{A_i \in \mathbb{R}^2 : i \in \mathbb{N}_+\}, \quad (5)$$

where A_i denotes AP i and its location. Note that we consider the urban scenario that $\lambda_u \geq \lambda_a$ since it is more convenient to deploy UAVs in such an environment.

The quality of a wireless link between a UAV and the typical AP highly depends on whether or not the wireless link is line-of-sight (LoS). An LoS link between two spatial points means that the link is not visually blocked from one point to the other. To model the LoS probability of a wireless link between the typical AP and a UAV, we adopt the following LoS probability model for a low-altitude platform proposed in [12]:

$$\rho(\Theta) \triangleq \frac{1}{1 + c_2 \exp(-c_1 \Theta)}, \quad (6)$$

where $\Theta \triangleq \tan^{-1}(H_i/\|X_i\|)$ is the elevation angle of U_i observed from the typical AP, c_1 and c_2 are the environment-related positive coefficients (for rural, urban, etc.). Suppose each UAV is positioned at the same altitude H_o and associates with an AP according to the following scheme:

$$A_\star \triangleq \arg \max_{i: A_i \in \Phi_a} L_i(H_o^2 + \|A_i\|^2)^{-\frac{\alpha}{2}}, \quad (7)$$

where $\alpha > 2$ denotes the path loss exponent and $L_i \in \{1, \ell\}$ is the LoS gain of AP A_i that is a Bernoulli random variable equal to one if the link between U_i and the A_i is LoS and equal to $\ell \in [0, 1]$ otherwise. Note that in this AP association scheme, the transmit power of the AP is not considered in that all the APs have the same transmit power and the channel fading effect is averaged out.

³This 3D point process is a generalization of the 3D point process proposed in our previous work [11] by considering a general distribution of the altitude of each UAV.

B. Analysis for Uplink Outage Probability

In this subsection, we focus on the analysis of the uplink outage probability. To facilitate the derivation of the outage probability, we need to first introduce two related theorems in the following. The first theorem is about the distribution of the path loss of the link from a UAV to its associating AP, which is shown in the following.

Theorem 1. *Let L_\star and $\|A_\star\|$ denote the LoS gain and distance between each UAV and its associating AP. Define $R_\star(r) \triangleq \mathbb{P}[L_\star \|A_\star\|^{-\alpha} \leq r]$ and it can be found as*

$$R_\star(r) = \exp(-\pi \lambda_a \Upsilon(r)), \quad (8)$$

where $\Upsilon(\cdot)$ is defined as

$$\begin{aligned} \Upsilon(r) \triangleq & \int_0^{\left[\left(\frac{1}{r}\right)^{\frac{2}{\alpha}} - H_o^2\right]^+} \rho(\vartheta_y) dy \\ & + \int_0^{\left[\left(\frac{1}{r}\right)^{\frac{2}{\alpha}} - H_o^2\right]^+} (1 - \rho(\vartheta_y)) dy. \end{aligned} \quad (9)$$

$[x]^+ \triangleq \max\{0, x\}$, and $\vartheta_y \triangleq \tan^{-1}(H_o/\sqrt{y})$.

Proof: See Appendix A. ■

R_\star in Theorem 1 inherits the properties from the UAV association scheme in (7). Note that $\Upsilon(r)$ is a decreasing function wherein the upper limit of the integral is not zero. Let I_{ul} be the interference power received by the typical AP⁴, and can be written as

$$I_{ul} \triangleq \sum_{i: U_i \in \tilde{\Phi}_u \setminus U_\star} g_i L_i \|U_i\|^{-\alpha}, \quad (10)$$

where U_\star is the reference UAV and $\tilde{\Phi}_u$ is the set of UAVs from other cells using the same resource block as U_\star . $g_i \sim \exp(1)$ is the uplink channel fading gain and is assumed to be i.i.d. and independent to L_i and U_i . The following theorem shows the Laplace transform of I_{ul} .

Theorem 2. *If the Laplace transform of I_{ul} is defined as $\mathcal{L}_{I_{ul}}(s) \triangleq \mathbb{E}[\exp(-sI_{ul})]$ for $s > 0$, it can be found as*

$$\mathcal{L}_{I_{ul}}(s) = \exp\left(-\pi \lambda_a \int_0^\infty \mathcal{I}_g(sy^{-\frac{\alpha}{2}}, \vartheta_y) dy\right), \quad (11)$$

where $\mathcal{I}_g(u, w)$, for $u, w > 0$, is defined as

$$\begin{aligned} \mathcal{I}_g(u, w) \triangleq & \rho(w)[1 - \mathcal{L}_g(u \cos^\alpha(w))] \\ & + (1 - \rho(w))[1 - \mathcal{L}_g(\ell u \cos^\alpha(w))]. \end{aligned} \quad (12)$$

Proof: See Appendix B. ■

Theorem 2 indicates how the uplink interference is affected by the deployments of UAVs and APs and the LoS channel impact. Note that (11) is a function of the density of APs λ_a since we assume that only one UAV in each cell is allowed to transmit in a time slot so that the density of $\tilde{\Phi}_u$ is equal to λ_a . Theorem 2 helps derive the uplink outage probability as

⁴According to the Slivnyak theorem [13], the statistical properties evaluated at any particular point in homogeneous PPPs are the same.

TABLE I
NETWORK PARAMETERS FOR SIMULATION

Parameter	Value
UAV Density λ_u (UAVs/m ²)	1×10^{-5}
AP Density λ_a (APs/m ²)	$\lambda_u/[10, 300]$
UAV Height H_o (m)	100
SIR Threshold η	0.5
Path-loss Exponent α	2.75
(c_1, c_2) in (6) for urban	(0.1581, 43.9142)
Channel Attenuation Gain of NLoS ℓ	0.25
Training Data Size for Each UAV $ D_i $	20
Number of clients C	10, 30, 50
Pre-designated Training Round T	200

defined in the following. The signal-to-interference ratio (SIR) at the typical AP in Fig. 1(b) is defined as

$$\gamma \triangleq \frac{G_* L_* \|A_*\|^{-\alpha}}{I_{ul}}, \quad (13)$$

where G_* is the channel fading gain from the reference UAV. Here we define the uplink outage probability of a UAV as

$$p_{out} = \mathbb{P}[\gamma \leq \eta] = \mathbb{P}\left[\frac{G_* L_* \|A_*\|^{-\alpha}}{I_{ul}} \leq \eta\right], \quad (14)$$

and η is the SIR threshold for successful decoding. According to the previous theorems, we can achieve the uplink outage probability as follows.

Theorem 3. *If the uplink outage probabilities of all UAVs at any training round are independent, the uplink outage probability is explicitly found as*

$$p_{out} = 1 - \mathbb{E}_{R'_*} \left\{ \exp \left(-\pi \lambda_a \int_0^\infty \mathcal{I}_g \left(\frac{\eta y^{-\frac{\alpha}{2}}}{R'_*}, \vartheta_y \right) dy \right) \right\}. \quad (15)$$

$R'_*(r) = \frac{dR_*(r)}{dr}$ is the power density function (PDF) of R_* written as

$$R'_*(r) = -\pi \lambda_a \Upsilon'(r) \exp(-\pi \lambda_a \Upsilon(r)). \quad (16)$$

Proof: According to the uplink outage probability defined in (14), the uplink outage probability can be rewritten as

$$p_{out} = \mathbb{P} \left[G_* \leq \frac{\eta I_{ul}}{L_* \|A_*\|^{-\alpha}} \right] = 1 - \mathcal{L}_{I_{ul}} \left(\frac{\eta}{L_* \|A_*\|^{-\alpha}} \right).$$

By applying Theorems 1 and 2, the result (15) is readily obtained. ■

As shown in Fig. 2(c), the uplink outage probability increases as λ_u/λ_a increases since more interference is induced. In the following section, we will demonstrate the numerical results and discuss how deployments of the UAVs and APs affect such an FL algorithm that models the outage of data delivery between the UAV and its associating AP proposed in Sec. II.

IV. NUMERICAL RESULTS AND DISCUSSIONS

In this section, we investigate the proposed FL model over a cellular-connected UAV network. The MNIST dataset is also adopted for the simulation in this section, as the simulation performed in Section II-B. The main difference between the simulations in this section and those in Section II-B is that

uplink transmission outages that depend on the deployment densities of the UAVs and the APs are considered in the simulations here whereas they were not affected by the deployment densities of the UAVs and the APs of the simulations in Section II-B. Namely, the uplink outages of all the UAVs clients are now affected by the UAV and AP densities. All the UAVs associate with their APs using the scheme in (7) and they would like to jointly learn a global model with the ES through the proposed FL model.

The simulation results and discussions in this section aim to achieve two goals. The first goal is to illustrate how the learning accuracy is affected by the UAV and AP deployments and the second one is to see whether learning accuracy can be estimated by Fig. 2. The second goal is to observe whether or not λ_u/λ_a can be used to estimate the learning accuracy through p_{out} by a series of mapping, i.e., $\lambda_u/\lambda_a \rightarrow p_{out} \rightarrow$ learning accuracy, and we want to know how precisely the estimation can be made when compared to the opposite simulation scenario where the UAVs and APs are deployed in a large-scale network⁵. As can be seen in Figs. 2(b) and (c), for example, when λ_u/λ_a is 70, its corresponding uplink outage probability p_{out} is 0.6, and the learning accuracy the around 0.68 when number of clients $C = 10$ with non-i.i.d. datasets according to the figure.

Fig. 3 shows the simulation results of the proposed FL model over a cellular-connected UAV network in which the UAVs and APs are deployed in a large area. As illustrated in the figure, the mapping estimation mentioned previously is fairly precise when it is compared with its corresponding simulated counterparts. Moreover, it shows that the UAV and AP deployment densities affect the uplink outages, which lead to intermittent updates in FL and accuracy degradation as pointed out in previous section. Straightforwardly, the uplink outage is more likely to happen as λ_u/λ_a increases due to more interference induced and/or larger transmission distance between an AP and a UAV. Also, the learning accuracy is affected by the number of clients, i.e., C . When λ_u/λ_a is low, C needs to be small in order to achieve a high learning accuracy, yet an excessively large C leads to overfitting and yields diminishing returns accordingly. On the other hand, when λ_u/λ_a is high, C should be large in order to compensate the accuracy degradation caused by intermittent updates due to uplink transmission outages.

V. CONCLUSION

In the literature, the studies of FL over wireless communication were mainly conducted based on two unrealistic assumptions, that is, no transmission outages between clients and a server and no data heterogeneity among all wireless clients. Such studies cannot practically reflect the accurate performance of FL when employing FL to accomplish a learning job in wireless networks. To practically understand the impacts of data delivery outage on FL, we propose and

⁵The discussions in this section focus on the case of the UAV clients with non-i.i.d. datasets, whereas this mapping estimation can also be implemented in the case of the UAV clients with i.i.d. datasets.

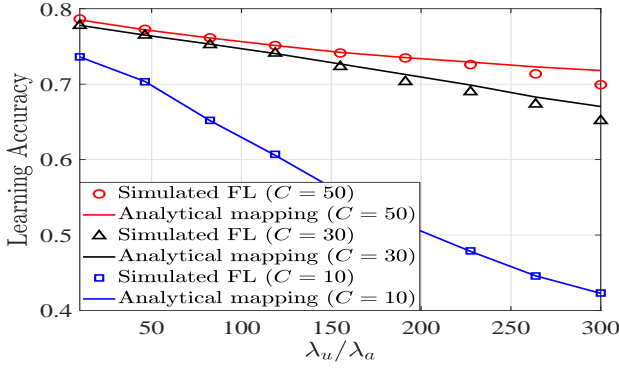


Fig. 3. Simulation results of the learning accuracy of the proposed FL model for the case of non-i.i.d. datasets at the UAV clients.

evaluate an FL model that is able to characterize transmission outages in a cellular-connected UAV network consisting UAV clients with non-iid datasets. A tractable approach to analyzing the uplink outage probability is proposed and the uplink outage probability of the UAV is explicitly derived in a neat form, which paves the way to evaluate the convergence performance of the proposed FL model. The estimation is fairly accurate and provides insights into how to properly deploy the UAVs and APs so as to achieve the accuracy requirement of the proposed FL model.

APPENDIX

A. Proof of Theorem 1

According to the definition of R_* , $R_*(r)$ can be explicitly written as

$$\begin{aligned}
 R_*(r) &\stackrel{(a)}{=} \mathbb{P} \left[\max_{i:A_i \in \Phi_a} \left\{ \frac{L_i}{\left[\|A_i\|^2 + H_o^2 \right]^{\frac{\alpha}{2}}} \right\} \leq r \right] \\
 &\stackrel{(b)}{=} \mathbb{E} \left\{ \prod_{i:A_i \in \Phi_a} \mathbb{P} \left[\frac{L_i}{\left[\|A_i\|^2 + H_o^2 \right]^{\frac{\alpha}{2}}} \leq r \right] \right\} \\
 &\stackrel{(c)}{=} \exp \left(-2\pi\lambda_a \int_0^\infty \mathbb{P} \left[\frac{L}{\left[x^2 + H_o^2 \right]^{\frac{\alpha}{2}}} > r \right] x dx \right),
 \end{aligned}$$

where (a) inherits the property from (7) since signal attenuation is equivalent in the downlink and uplink, (b) follows from the fact that all $L_i/(\|A_i\|^2 + H_o^2)^{\alpha/2}$'s are independent, and (c) is obtained by applying probability generating functional (PGFL) of a Homogeneous PPP to Φ_a . The subscript i of L_i is dropped for simplifying notation, and this is applied in the following of this paper. substitute x^2 as y and let $\vartheta_y = \tan^{-1}(H_o/\sqrt{y})$, the inner term $\mathbb{P} [L/[y + H_o^2]^{\alpha/2} > r]$ can be rewritten as

$$\begin{aligned}
 \mathbb{P} \left[\frac{L}{\left[y + H_o^2 \right]^{\frac{\alpha}{2}}} > r \right] &= \rho(\vartheta_y) \mathbb{P} \left[\frac{1}{\left(y + H_o^2 \right)^{\frac{\alpha}{2}}} > r \right] \\
 &+ [1 - \rho(\vartheta_y)] \mathbb{P} \left[\frac{\ell}{\left(y + H_o^2 \right)^{\frac{\alpha}{2}}} > r \right] = \rho(\vartheta_y) \mathbb{P} \left[y < \left(\frac{\ell}{r} \right)^{\frac{2}{\alpha}} \right. \\
 &\left. - H_o^2 \right] + [1 - \rho(\vartheta_y)] \mathbb{P} \left[y < \left(\frac{\ell}{r} \right)^{\frac{2}{\alpha}} - H_o^2 \right],
 \end{aligned}$$

and $\Upsilon(r)$ and R_* are subsequently obtained.

B. Proof of Theorem 2

According to the definition of I_{ul} , its Laplace transform is given by

$$\begin{aligned}
 \mathbb{E} [e^{-sI_{ul}}] &= \mathbb{E} \left[\prod_{i:U_i \in \Phi_u \setminus U_*} \exp \left(-sg_i L_i \left(\|X_i\|^2 + H_o^2 \right)^{-\frac{\alpha}{2}} \right) \right] \\
 &\stackrel{(a)}{=} \exp \left(-\pi\lambda_a \int_0^\infty \left\{ 1 - \mathbb{E} \left[e^{-\frac{sgL}{\|y+H_o^2\|^{\alpha/2}}} \right] \right\} dy \right) \\
 &\stackrel{(b)}{=} \exp \left(-\pi\lambda_a \int_0^\infty \mathbb{P} \left[Z \leq \frac{sgL}{\|y+H_o^2\|^{\alpha/2}} \right] dy \right),
 \end{aligned}$$

where (a) is obtained by applying the PGFL of a homogeneous PPP to the projections of Φ_u and (b) is obtained by the CDF of a random variable $Z \sim \exp(1)$, i.e., $\mathbb{P}[Z \leq z] = 1 - e^{-z}$. Let $\vartheta_y = \tan^{-1}(H_o/\sqrt{y})$ and we get

$$\begin{aligned}
 \mathbb{P} \left[Z \leq \frac{sgL}{\|y+H_o^2\|^{\alpha/2}} \right] &= \rho(\vartheta_y) \mathbb{P} \left[Z \leq \frac{sg}{\|y+H_o^2\|^{\alpha/2}} \right] \\
 &+ (1 - \rho(\vartheta_y)) \mathbb{P} \left[Z \leq \frac{sg\ell}{\|y+H_o^2\|^{\alpha/2}} \right].
 \end{aligned}$$

Replacing $\|y + H_o^2\|^{\alpha/2}$ with $y^{\alpha/2} \sec^{\alpha}(\vartheta_y)$ in the expression of $\mathcal{L}_{I_{ul}}(s)$ yields the outcome in (11).

REFERENCES

- [1] X. Wang, Y. Han, C. Wang, Q. Zhao, X. Chen, and M. Chen, "In-Edge AI: Intelligentizing mobile edge computing, caching and communication by federated learning," *IEEE Network*, vol. 33, no. 5, pp. 156–165, Jul. 2019.
- [2] Q. Yang, Y. Liu, Y. Cheng, Y. Kang, T. Chen, and H. Yu, *Federated Learning*, 1st ed. Morgan and Claypool, 2019.
- [3] S. Niknam, H. S. Dhillon, and J. H. Reed, "Federated learning for wireless communications: Motivation, opportunities, and challenges," *IEEE Commun. Mag.*, vol. 58, no. 6, pp. 46–51, Jun. 2020.
- [4] F. Sattler, S. Wiedemann, K. R. Müller, and W. Samek, "Robust and communication-efficient federated learning from non-i.i.d. data," *IEEE Trans. Neural Netw. Learn. Syst.*, vol. 31, no. 9, pp. 3400–3413, Sep. 2020.
- [5] S. Wang, T. Tuor, T. Salonidis, K. K. Leung, C. Makaya, T. He, and K. Chan, "Adaptive federated learning in resource constrained edge computing systems," *IEEE J. Select. Areas Commun.*, vol. 37, no. 6, pp. 1205–1221, Mar. 2019.
- [6] M. M. Amiri and D. Gündüz, "Federated learning over wireless fading channels," *IEEE Trans. Wireless Commun.*, vol. 19, no. 5, pp. 3546–3557, Feb. 2020.
- [7] Y.-S. Jeon, M. M. Amiri, J. Li, and H. V. Poor, "A compressive sensing approach for federated learning over massive MIMO communication systems," *IEEE Trans. Wireless Commun.*, vol. 20, no. 3, pp. 1990–2004, Nov. 2021.
- [8] G. Zhu, Y. Du, D. Gündüz, and K. Huang, "One-bit over-the-air aggregation for communication-efficient federated edge learning: Design and convergence analysis," *IEEE Trans. Wireless Commun.*, vol. 20, no. 3, pp. 2120–2135, Nov. 2021.
- [9] G. Zhu, Y. Wang, and K. Huang, "Broadband analog aggregation for low-latency federated edge learning," *IEEE Trans. Wireless Commun.*, vol. 19, no. 1, pp. 491–506, Oct. 2020.
- [10] Q.-V. Pham, M. Zeng, R. Ruby, T. Huynh-The, and W.-J. Hwang, "UAV communications for sustainable federated learning," *IEEE Trans. Veh. Technol.*, vol. 70, no. 4, pp. 3944–3948, Mar. 2021.
- [11] C.-H. Liu, D.-C. Liang, and R.-H. Gau, "A 3D tractable model for UAV-Enabled cellular networks with multiple antennas," *IEEE Trans. Wireless Commun.*, pp. 1–17, Early Access 2021.
- [12] A. Al-Hourani, S. Kandeepan, and S. Lardner, "Optimal LAP altitude for maximum coverage," *IEEE Trans. Wireless Commun.*, vol. 3, no. 6, pp. 569–572, Dec. 2014.
- [13] F. Baccelli and B. Błaszczyszyn, *Stochastic Geometry and Wireless Networks: Volume I Theory*. Now Foundations and Trends, 2010.